

Anisotropy of magnetic interactions and symmetry of the order parameter in unconventional superconductor Sr_2RuO_4

Bongjae Kim^{1,*}, Sergii Khmelevskyi^{1,2*}, I. I. Mazin³, D. F. Agterberg⁴, and Cesare Franchini^{1†}

¹ *University of Vienna, Faculty of Physics and Center for Computational Materials Science, Vienna A-1090, Austria*

² *Center for Computational Materials Science, Institute for Applied Physics, Vienna University of Technology, Wiedner Hauptstrasse 8 - 10, 1040 Vienna, Austria*

³ *Code 6393, Naval Research Laboratory, Washington, D.C. 20375, USA and*

⁴ *Department of Physics, University of Wisconsin, Milwaukee, Wisconsin 53201, USA*
(Dated: July 2, 2022)

We present a density-functional based analysis of magnetic interactions in Sr_2RuO_4 and discuss the role of magnetic anisotropy in its unconventional superconductivity. Our goal is twofold. First, we access the possibility of the superconducting order parameter rotation in an external magnetic field of 200 Oe, and conclude that the spin-orbit interaction in this material is several orders of magnitude too strong to be consistent with this hypothesis. Thus, the observed invariance of the Knight shift across T_c has no plausible explanation, and casts doubt on using the Knight shift as an ultimate litmus paper for the pairing symmetry. Second, we propose a quantitative double-exchange-like model for combining itinerant fermions with a Heisenberg–Kitaev magnetic Hamiltonian. This model is complementary to the Hubbard-model-based calculations published so far, and forms an alternative framework for exploring superconducting symmetry in Sr_2RuO_4 . As an example, we use this model to analyze the degeneracy between various p -triplet states in the simplest mean-field approximation, and show that it splits into a single and two doublets with the ground state defined by the competition between the so-called “Kitaev” and “compass” terms.

Superconductivity in Sr_2RuO_4 , even though it occurs at a rather low temperature, has been attracting attention comparable to that attached to high-temperature superconductors [1]. For many years the dominant opinion was that it represents a unique example of a chiral triplet pairing state [2–5]. Interestingly, the original premise that led to this hypothesis was presumed proximity of Sr_2RuO_4 to ferromagnetism, and thus it was touted as a 3D analogue of ^3He [6, 7]. It was soon discovered, first theoretically [8], and then experimentally [9], that the leading instability occurs in an antiferromagnetic, not ferromagnetic channel, and thus a spin-fluctuation exchange in the BCS-Schrieffer spirit would normally lead to a d -wave, not p -wave superconductivity.

The issue seems to have been decided conclusively when the Knight shift on Ru was shown to be temperature-independent across T_c [2], and later also on

O [3], and the neutron-measured spin-susceptibility was found to be roughly constant across the transition as well [4]. The chiral p -wave state with an order parameter $\mathbf{d} = \text{const}(x + iy)\hat{\mathbf{z}}$, where the Cooper pair spins can freely rotate in-plane, is the only state that could have this property. Moreover, since in this state spins are confined in the xy plane, the Knight shift in a magnetic field parallel to $\hat{\mathbf{z}}$ is supposed to drop below T_c in pretty much the same manner as in singlet superconductors. Nonetheless, when eventually this experiment was performed [10], it appeared that K_z is also independent of temperature. The authors of Ref. [10] attempted to reconcile the accepted pairing symmetry with their experiment, by assuming that the experimental magnetic field of 200 Oe is affecting drastically the pairing state and converting it to $\mathbf{d} = \text{const}(x + \alpha iz)\hat{\mathbf{y}}$ (with or without admixture of the partner $x \leftrightarrow y$ state), with $\alpha \approx 1$. One goal of our paper is to estimate whether this hypothesis is tenable with realistic material parameters.

It is worth noting that the invariance of the in-plane susceptibility is the only experiment consistent *exclusively* with a chiral p -state (CpS). Some probes indicate chirality (μSR detects spontaneous currents below T_c [5]), while others indicate breaking of time-reversal symmetry [11], but the triplet parity is not, in principle, necessary to explain these experiments. For instance, the singlet chiral state $\Delta = \text{const}(xz + iyz)$, or even $\Delta = \text{const}(x^2 + y^2 + i\alpha xy)$, which is not chiral (although this second state would require two phase transitions with decreasing temperature, which has never been detected), but breaks the time reversal symmetry, are other admissible candidates. Josephson junction experiments [12] suggested that the order parameter changes sign under the $(x, y) \leftrightarrow (-x, -y)$ transformation, which is consistent with a CpS, but also with other order parameters [13].

Spin-orbit coupling plays an important role not only in selecting between different triplet state (chiral vs. helical), but also in the structure of the chiral state itself. For instance, in $\text{Cu}_x\text{Bi}_2\text{Se}_3$, instead of the expected chiral state, a nematic spin-triplet state was observed [14, 15]. Indeed, in $\text{Cu}_x\text{Bi}_2\text{Se}_3$ the large spin-orbit coupling necessarily implies that a $\mathbf{d} = \text{const}(x + iy)\hat{\mathbf{z}}$ induces also an in-plane \mathbf{d} -vector component $\text{const}(\hat{\mathbf{x}} + i\hat{\mathbf{y}})z$ [16]. This in-plane component leads to a non-unitary pairing state,

which is not energetically favored in weak coupling [17], and, instead, the lower-symmetry nematic state with $\mathbf{d} = c_1 x \hat{\mathbf{z}} + c_2 z \hat{\mathbf{x}}$ is realized. In principle, similar physics must occur in Sr_2RuO_4 , but there the corresponding induced in-plane \mathbf{d} -vector component should be much smaller, thus allowing for a chiral p -wave state to exist. However, this is a quantitative, not qualitative difference, and needs a better understanding of the role of spin-orbit coupling.

Finally, recent years have brought about an array of experiments that are actually *inconsistent* with the CpS . One prediction of a CpS is the existence of edge states at boundaries and at domain walls [18–20]. However, no evidence for these edge states has been found [19, 21]. There are a variety of predictions about the response of CpS to in-plane magnetic fields that have not been observed experimentally. In particular, it is known that a finite in-plane magnetic field should lead to two superconducting transitions as temperature is reduced [22, 23] and that the slope of the upper critical field with temperature at T_c should depend upon the in-plane field direction (this is only true for pairing states that can break time-reversal symmetry) [23, 24]. In addition, several different probes indicate behavior resembling substantial Pauli paramagnetic effects (see Ref. [25] for discussion and original references). The latest cloud on the CpS sky appeared because of the uniaxial strain experiments. For the CpS (or, in fact, any other two-component state) the critical temperature, T_c , under an orthorhombic stress must change linearly with the strain (the $x\hat{\mathbf{z}}$ and $y\hat{\mathbf{z}}$ state are not degenerate any more, and the splitting is linear in strain). In the experiment [26] T_c varies at least quadratically (more likely, quartically), whereas the linear term is absent within the experimental accuracy. Moreover, it was established that the T_c variation traces the changes in the density of states, and peaks when the Fermi level passes the van Hove singularities at the X or Y points. This observation is particularly important, because, by symmetry, the superconducting gap in a triplet channel in a tetragonal superconductor is identically zero at X and Y (it need not be zero at a finite k_z , but in a highly 2D material like Sr_2RuO_4 it will be still very small by virtue of continuity). Correspondingly, one expects these van Hove singularities to have little effect on superconductivity. A slightly more subtle, but even more convincing argument against triplet pairing in Ref. [26] is related to the reduced critical field anisotropy. Finally, a recent detailed study of thermal conductivity has concluded that a d -wave state is by far better consistent with the thermal transport than the CpS [27].

In fact, only one fact unambiguously points toward the CpS : the invariance of the spin susceptibility in the in-plane magnetic field — but, as discussed above, the analogous experiment for the out-of-plane field *also* show such an invariance. Thus, our acceptance of the NMR data as an ultimate proof of the CpS hinges upon the

possibility of a magnetic field of 200 Oe (0.02 T, or 13 mK in temperature units) to overcome the energy difference between the helical ($\mathbf{d} \perp \hat{\mathbf{z}}$) and chiral ($\mathbf{d} \parallel \hat{\mathbf{z}}$) states. One can show (the derivation is presented below) that this implies that the two states, whose energy difference comes from the spin-orbit (SO) interaction, are nearly degenerate with the accuracy $\delta \approx 10^{-7} \text{ K} \approx 10^{-10} \lambda$, where $\lambda \approx 200 \text{ meV}$ is the SO constant. Moreover, it is often claimed that the solution of other paradoxes outlined above may be obtained (although nobody has convincingly succeeded in that) in a formalism where the relativistic effects would be fully accounted for since the separation between singlet and triplet channels is only possible in terms of the full angular momentum, rather than just electron spins.

In order to illustrate how SO coupling affects the core assumption of the field-induced \mathbf{d} -vector rotation, let us show a simple back-of-the-envelope calculation: suppose that the one-electron Hamiltonian has a relativistic term of the order of κM_z^2 . The physical meaning of this term is that in the *normal* state when n electron spins are confined in the xy plane (as opposed to be parallel to z), this affects the exchange part of the effective crystal potential, and, correspondingly, one-electron energies. The change is proportional to n , and so is the number of affected one-electron states, leading to an energy loss of the order of κn^2 , where κ is the magnetic anisotropy scale which is determined by the SO coupling. One way in which this energy contribution manifests itself is the conventional magnetic anisotropy in a spin-ordered state in which case $n \approx M/\mu_B$. However, the same “feedback” effect must be present in a triplet superconducting state. The number of electrons bound in Cooper pairs and thus forced to be either parallel or perpendicular to z can be estimated as $n \sim \Delta N$, where Δ is some average superconducting gap, and N is the density of states, which has been experimentally measured to be about 8 states/spin/Ru/eV [1]. Assuming $\Delta \sim 15 \text{ K}$, we estimate $n \sim 0.01 \text{ e/Ru}$. If the magnetic anisotropy scale κ is of the order of 10 K (we will show later that this is the case), then the total energy loss incurred by rotating the spins of the Cooper pairs is $\Delta E_{sc} \approx 10^{-3} \text{ K}$. This seems like a small number, but we shall compare it with the energy gained by allowing magnetic screening of an external field of 200 Oe, which is $\Delta E_{mag} \approx B^2 N \approx 10^{-7} \text{ K}$. This is *four orders of magnitude* smaller than the estimated loss of superconducting energy. In other words, to allows for the presumed d -vector rotation, various relativistic effects must fortuitously cancel each other with a 10^{-4} accuracy.

This simple estimate emphasizes the importance of getting a handle of the type and scale of relativistic effects in Sr_2RuO_4 . So far all efforts in this direction have been performed either within simplified models or by educated guesses from the experiment [20, 28–30]. The goal of this paper is to address the issue from a first principle perspective. We shall demonstrate reliability of this ap-

proach by computing the *ab initio* SO coupling constant λ and comparing it with the experiment, and by comparing the Fourier transform of the calculated exchange interaction with the experimentally measured \mathbf{q} -dependent spin susceptibility. The only serious problem with this approach is that it overestimates the tendency to magnetic ordering for a given set of magnetic interactions because of the mean field nature of the density functional theory. Thus we start with a realistic paramagnetic state of Sr_2RuO_4 , using the alloy analogy model in the first principles DFT framework and calculate the isotropic exchange interactions (See Methods). The Fourier transform of those gives us the shape of the full spin susceptibility in the momentum space; as expected, this is peaked at the nesting vector $\mathbf{q}_3 = (1, 1, 0)\frac{2\pi}{3a}$, in agreement with the experiment. Next, we calculate the mean-field energy of several ordered magnetic states, all characterized by the same wave vector $\mathbf{q}=\mathbf{q}_3$, and degenerate without SO interaction. This shall allow us to extract single-site and Kitaev nearest-neighbor relativistic terms (see below). Finally, we calculate magnetic anisotropy for the $\mathbf{q}=(1, 0, 0)\frac{\pi}{a}$ states, which breaks the tetragonal symmetry, and from there we extract the nearest neighbor compass exchange (See Methods). The energy scale of magnetic anisotropy appears rather large, which not only renders the hypothesis of a \mathbf{d} -vector rotation unlikely, but also supports the idea that anisotropic interactions must be properly accounted for before drawing conclusions from the experiment. The set of interactions that we derived should serve as a launching pad and testbed for model calculation of the superconducting properties. We maintain that a model where all interelectron interactions are absorbed into spin-spin interactions (with Hund's coupling between the spins and noninteracting electrons) is complementary to the widely used Hubbard model and at least as realistic.

Experimentally, Sr_2RuO_4 shows no sign of magnetic ordering down to the low temperatures. However, neutron diffraction studies have revealed [9, 31–33] spin fluctuations in the paramagnetic state with a characteristic nearly-commensurate wave vector $\mathbf{q} = (0.3, 0.3, 0)\frac{2\pi}{a}$, close to $\mathbf{q}_3 = (1, 1, 0)\frac{2\pi}{3a}$, which persist even at the room temperature [34]. The Density Functional Theory (DFT), being a static mean field theory (by some criteria, the best such theory possible), overestimates the tendency to magnetism. In its Generalized Gradient Approximation flavor (GGA) DFT stabilizes even ferromagnetic order, albeit with small moments [35]. Unsurprisingly, spin density waves with $\mathbf{q} = \mathbf{q}_3$ are even lower in energy. This deficiency of the DFT can, however, be put to a good use by mapping the DFT (*i.e.*, mean-field) energetics onto a spin-Hamiltonian, as it is often done, for instance, for Fe-based superconductors [36].

First we have calculated the Heisenberg part of the

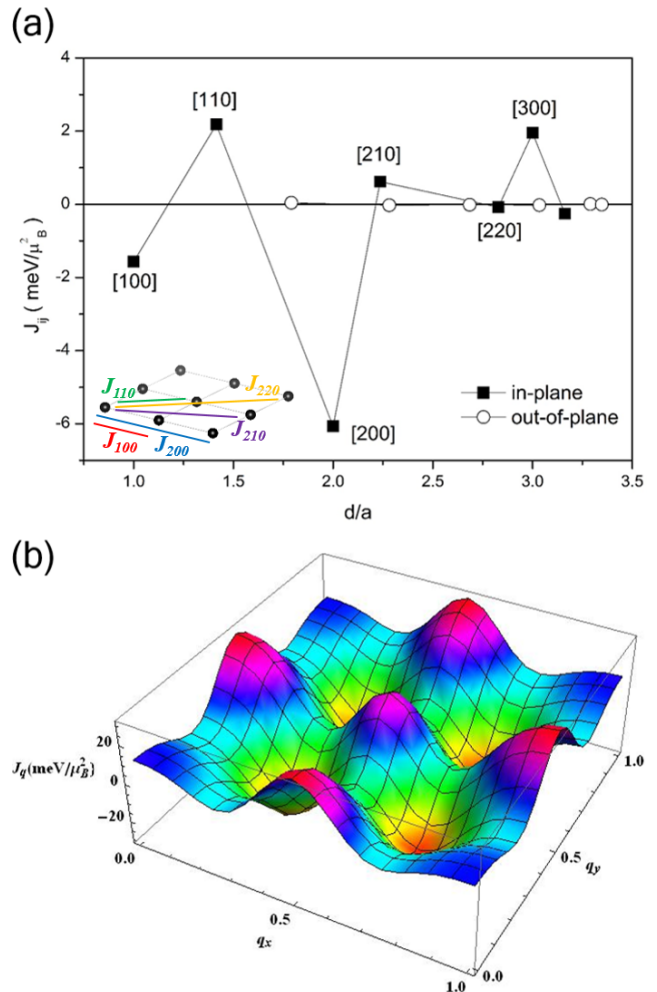


FIG. 1: **Calculated exchange interactions up to the 7th coordination sphere in Sr_2RuO_4 .** (a) The distance dependence (in terms of planar lattice constant) of isotropic exchange interactions for in-plane (filled square) and out-of-plane (open circle). (b) The Fourier transform of the exchange interactions shown in the panel (a).

Hamiltonian, defined as

$$H_H = - \sum_{\langle i \neq j \rangle} J_{ij} \mathbf{M}_i \cdot \mathbf{M}_j, \quad (1)$$

where \mathbf{M}_i is the Ru moment on the site i , and summation is performed over all bonds up to a given coordination sphere. The parameters are calculated in the Disordered Local Moments (DLM) approximation [37], which is used to model the paramagnetic state of Sr_2RuO_4 (See Methods for more details and employed approximations).

The results presented in the Fig. 1 are derived for the Ru local moment being fixed to $1 \mu_B$ in the DLM state. The obtained values of the exchange constants, however, are fairly independent on the values of the local moment fixed in the DLM state; the minimum of

the Fourier transform is always at $\mathbf{q} = (\alpha, \alpha, 0)$ with $\alpha = 0.3 - 0.31$. Note that the interplane exchanges nearly vanish, indicating an almost perfect 2D character of the magnetism in Sr_2RuO_4 . For instance, the nearest neighbors between-the-planes $J_{001} \approx 0.5 - 1 \text{ K}/\mu_B^2$ (ferromagnetic), or about $-0.01J_{200}$.

The leading term is the in-plane third nearest neighbour (NN) antiferromagnetic interaction J_{200} , which is quite counterintuitive from the point of view of the Hubbard model and superexchange mechanism that is often employed as a starting point. This is a consequence of the Ru electrons itinerancy, since Sr_2RuO_4 is a metal. The lattice Fourier transform, $J(\mathbf{q})$, of the calculated interactions is shown in the Figure 1 (b). $J(\mathbf{q})$ has a meaning of a measure of the energy ($J(\mathbf{q}) \cdot M^2$) of the spin-density fluctuations with a wave-vector \mathbf{q} and a given amplitude M [the quantity that is directly related to the static zero-temperature spin susceptibility is $1/J(\mathbf{q})$] The deep minima of $J(\mathbf{q})$ at $\mathbf{q} = (0.31, 0.31, 0)\frac{2\pi}{a}$ suggest that the spin-fluctuations with the wave vector \mathbf{q} will be dominant in the paramagnetic state of Sr_2RuO_4 . The position of these minima is indeed in perfect agreement with the sharp maxima of the integrated magnetic scattering intensity, experimentally observed in neutron diffraction [34]. Thus, both our calculation and the experiment suggest the dominance of the spin-fluctuations with the wave vector \mathbf{q}_3 in the excitation spectra of Sr_2RuO_4 .

In order to extract the relevant anisotropic exchange interaction parameters, we used direct calculations of the total energy in different magnetic configurations compatible with the ordering vector \mathbf{q}_3 . Note that anisotropic magnetic interactions appear exclusively due to the SO coupling (See Methods for the description of codes and approximations used in these calculations). Allowed anisotropic terms for the nearest neighbor terms are absorbed in the following Hamiltonian (simplified compared to a more complete expression discussed in the Methods section):

$$\begin{aligned} H_{rH} = & H_H + \sum_{\langle nn \rangle} J^{zz} M_i^z M_j^z \\ & + \sum_{\langle nnx \rangle} J^{xy} (M_i^x M_j^x - M_i^y M_j^y) \\ & + \sum_{\langle nny \rangle} J^{xy} (M_i^y M_j^y - M_i^x M_j^x), \end{aligned} \quad (2)$$

where the first term is given by Eq. 1, the second is sometimes called Kitaev interaction, and the last two represent the compass exchange. Summation in the last two terms is over all horizontal and all vertical bonds, respectively, while in the Kitaev term it is over all inequivalent bonds. Note that Dzyaloshinskii-Moriya terms [38, 39] are not allowed by symmetry.

The six most energetically favorable states are depicted in Fig. 2. The first three states can be described as har-

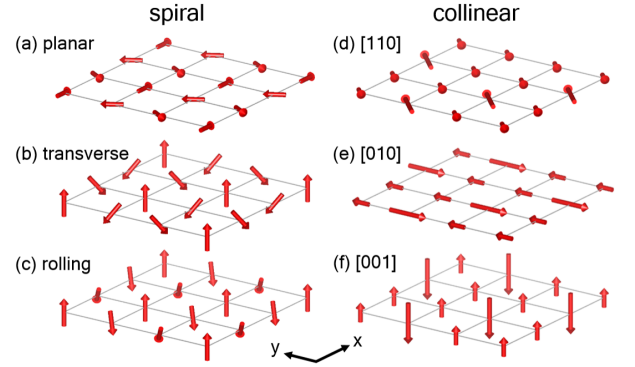


FIG. 2: **Lowest energy magnetic structures** ($\mathbf{q} = (1, 1, 0)\frac{2\pi}{3a}$) of RuO_2 basal plane in Sr_2RuO_4 . The (a)-(c) structures represent different types of spiral magnetic order and (d)-(f) corresponds to the collinear up-up-down magnetic order with different moment directions.

monic spin-density waves (SDWs):

$$\mathbf{M}_{ijk} = m\mathbf{A} \exp(-i\mathbf{R}_{ijk} \cdot \mathbf{q}_3), \quad (3)$$

where $\mathbf{A}_a = [-\frac{1}{2}, \frac{\sqrt{3}}{2}, 0]$, $\mathbf{A}_b = [\frac{i}{2\sqrt{2}}, -\frac{i}{2\sqrt{2}}, \frac{1}{2}]$, $\mathbf{A}_c = [\frac{i}{2\sqrt{2}}, \frac{i}{2\sqrt{2}}, \frac{1}{2}]$, with m hardly varying between the three states and equal to $0.76 \mu_B$. The fourth to sixth state are collinear where the amplitude of the moments varies along each of the crystallographic directions 100, 010, and 110 as $m', -m'/2, -m'/2$ (more precisely, $1.07, -0.56, -0.56 \mu_B$). Note that m' is very close to $\sqrt{2}m$ in the harmonic SDWs, and the average $\langle \mathbf{M}^2 \rangle$ is the same in all these states (within a 1.3% error). In this collinear state the direction of magnetization can be selected in three inequivalent ways, namely along 110, $\bar{1}\bar{1}0$ or 001. Upon inclusion of the SO term, the 001 collinear up-up-down structure is the ground state (Table I).

The difference between the scalar- and fully-relativistic calculations allows us to estimate the coupling constant λ [40–42]. A recent experimental estimation based on the resonant inelastic x-ray scattering (RIXS) gives $\lambda \approx 200 \text{ meV}$ [43]. Our estimation derived from the total energy difference between the relativistic and nonrelativistic total energies (E_{SOC} and E_{Nrel}), $\frac{3}{2}\lambda = E_{SOC} - E_{Nrel}$, gives $\lambda = 210 \text{ meV}$, in almost perfect agreement with the experiment.

Next, we fitted the energy differences in Table I to the Hamiltonian (2), extracting J^{zz} and J^{xy} (the fitting procedure included more parameters than in Eq. 2, and is discussed in the Methods Section). All isotropic (Heisenberg) parts of the exchange interactions are included in the H_H . The compass parameter J^{xy} does not affect the states with $\mathbf{q} \propto (1, 1, 0)$, and was extracted from a separate set of calculations with $\mathbf{q}_2 = (0, 1, 0)\frac{\pi}{a}$, and $\mathbf{M}_{ijk} = m\mathbf{A} \exp(-i\mathbf{R}_{ijk} \cdot \mathbf{q}_2)$, where $\mathbf{A}_\perp = (1, 0, 0)$ and $\mathbf{A}_\parallel = (0, 1, 0)$, and m was fixed to be equal to its value in

TABLE I: Calculated total energies (meV/Ru) of various states with the $\mathbf{q}_3 = (1, 1, 0)\frac{2\pi}{3a}$ periodicity. For spiral phases, the magnitude of the calculated local moments is $0.76\mu_B$, and for collinear up-up-down phase, $0.57\mu_B$ and $1.03\mu_S$ for up and down spin, respectively.

\mathbf{q}		spin orientation	energy
$(1, 1, 0)(2\pi/3a)$	spiral	planar	0
		rolling	-0.42
		transverse	-0.22
$(1, 1, 0)(2\pi/3a)$	collinear	(110)	-0.34
		(010)	-0.24
		(001)	-1.27
$(1, 0, 0)(\pi/a)$	collinear	(100)	38.06
	stripes	(010)	39.57

the spiral states, $0.76\mu_B$. These wave vectors define so-called single stripe antiferromagnetic order, well known in Fe-based superconductors.

Thus obtained parameters are $J^{zz} = 1.2 \pm 0.6 \text{ meV}/\mu_B^2$, and $J^{xy} = 1.0 \text{ meV}/\mu_B^2$ ($J^{zz}m^2 = 0.70 \pm 0.35 \text{ meV}$, $J^{xy} = 0.57 \text{ meV}$, for $m = 0.76\mu_B$). The details of fitting are described in the Methods section. Note that J^{xy} does not have an error bar not because it was accurately determined, but because we did not have enough calculations to estimate the error. First, one observes that the scale of the anisotropy induced by SO is of the order of 10 K. As discussed in the introduction, this renders the explanation of the invariance of the Knight shift below T_c in term of the order parameter rotation [10] untenable and shakes the main argument in favor of the chiral triplet superconductivity in Sr_2RuO_4 . Second, our fitting provides a powerful tool for modeling normal and especially superconducting properties of Sr_2RuO_4 from an entirely different angle. Compared to the generally accepted models based on the Hubbard-Hund Hamiltonians, our new approach is based entirely on first principles calculations, and emphasizes the role of magnetic interactions. The corresponding *DFT-inspired* model Hamiltonian reads

$$H = H_{rH} + H_e$$

$$H_e = \sum_{\mathbf{k}\alpha s} \varepsilon_{\mathbf{k}\alpha} c_{\mathbf{k}\alpha s}^\dagger c_{\mathbf{k}\alpha s} - I \sum_{\mathbf{k}\mathbf{q}\alpha s s'} c_{\mathbf{k}-\mathbf{q},\alpha s}^\dagger \mathbf{M}_{\mathbf{q}} \cdot \boldsymbol{\sigma}_{ss'} c_{\mathbf{k}\alpha s'}, \quad (4)$$

where the first term is the noninteracting energy, with the band (spin) indices α (s), and the second is the Hund's rule (Stoner, in the DFT parlance) coupling. All electron-electron interactions carried by spin fluctuations are absorbed in the local Hund's interaction I and the intersite magnetic interactions H_{rH} , while interactions due to charge fluctuations are not included in Eq. 4, but can be added separately, if needed (or just collected in one Coulomb pseudopotential μ^* , as in the Eliashberg theory). Eq. 4 can be understood as generalized double-

exchange one [44]. Indeed, this model, inspired by DFT calculations, entails electrons moving in the same effective potential as used in other techniques, and described by the same tight-binding parameters. However, as it is usual in DFT, all electron-electron interactions are implicitly integrated out. Instead, we introduce quasi-local magnetic moments that interact with the electrons via the local Hund's rule coupling (parameterized as the Stoner parameter in DFT), while the moments interact among themselves according to the sum of the long-range Heisenberg and the short-range anisotropic Hamiltonian (Eq. 2). The former part incorporates implicitly all Fermi surface effects, including nesting at $\mathbf{q} = \{0.3, 0.3, 0\}\frac{2\pi}{a}$, while the latter selects between different triplet states.

It might be instructive to demonstrate how Eq. 4 can be reduced to a Hamiltonian including only the itinerant electrons (as convenient for analyzing superconductivity). We can safely assume that all J s are much smaller than I , introduce the itinerant spin polarization $\mathbf{s}_{i\alpha} = \sum_{ss'} c_{i\alpha s}^\dagger \boldsymbol{\sigma}_{ss'} c_{i\alpha s'}$, and single out the terms relevant to the pairwise interaction between $\mathbf{s}_{i\alpha}$ and $\mathbf{s}_{j\beta}$:

$$E_{ij,\alpha\beta} = -I\mathbf{M}_i \cdot \mathbf{s}_{i\alpha} - I\mathbf{M}_j \cdot \mathbf{s}_{j\beta} - J_{ij}\mathbf{M}_i \cdot \mathbf{M}_j \quad (5)$$

In the lowest order in J , the mean field solution requires that \mathbf{M}_i and $\mathbf{s}_{i\alpha}$ be parallel, $E_{ij,\alpha\beta} = -2IM_s - J_{ij}M^2\hat{\mathbf{s}}_{i\alpha} \cdot \hat{\mathbf{s}}_{j\beta}$, and the effective pairwise interaction can be written as $-J_{ij}M^2\hat{\mathbf{s}}_{i\alpha} \cdot \hat{\mathbf{s}}_{j\beta}$ (note that essentially the same Hamiltonian, only written in the orbital basis rather than the band basis, which can also be done in this case, was applied to Fe-based superconductors in several papers, for instance, in Ref. [45]; after summation of the total energy over the band indices α, β these approaches become equivalent). In principle, one can easily derive the next order correction to the interaction, which is $+(J_{ij}^2 M^3 / I s)(\hat{\mathbf{s}}_{i\alpha} \cdot \hat{\mathbf{s}}_{j\beta})^2$.

As an example of how this Hamiltonian can be used to address superconductivity, we solve in the simplest mean field approximation the problem of the relative energetics of the five unitary p -triplet states. In particular, beginning with $H = -J_{ij}M^2\hat{\mathbf{s}}_{i\alpha} \cdot \hat{\mathbf{s}}_{j\beta}$ and restricting the electronic spins to a single band for simplicity (generalizing onto three bands with realistic dispersions is straightforward), we find that the Kitaev and compass exchange modify the pairing interaction δV in different pairing channels differently, as shown in Table II.

Thus, in this approximation the five states split into two planar doublets (of course, this degeneracy is not driven by symmetry, and will be lifted in more sophisticated calculations, but likely the splitting will be small) and a CpS singlet, which is located between the doublets if $J_{zz} < J_{xy}$ and below both of them otherwise. In other words, we have shown that selection between chiral and planar superconductivity is driven by the competition between the Kitaev and compass anisotropic exchange.

We reiterate that we do not insist that this approach is *superior* to the Hubbard Hamiltonian, but it is *different*

TABLE II: Relative change in pairing interaction for spin-triplet pairing channels due to Kitaev and compass exchange terms

Pairing Channel		$\delta V/2$
$(\sin k_x \pm i \sin k_y)\hat{z}$	axial chiral	J^{zz}
$\sin k_x \hat{x} + \sin k_y \hat{y}$	planar radial	$-J^{zz} + 2J^{xy}$
$\sin k_x \hat{y} + \sin k_y \hat{x}$	planar quadrupolar	$-J^{zz} - 2J^{xy}$
$\sin k_x \hat{x} - \sin k_y \hat{y}$	planar quadrupolar	$-J^{zz} + 2J^{xy}$
$\sin k_x \hat{y} - \sin k_y \hat{x}$	planar tangential	$-J^{zz} - 2J^{xy}$

ent and complementary, having the potential to uncover new physics. Similar to the former, it can be used in the contexts of, *e.g.*, random phase approximation (RPA), fluctuation exchange (FLEX) or functional renormalization group (fRG) calculations.

A final note relates to the recent experiments on strained Sr_2RuO_4 . This is a large topic mostly outside of the scope of this paper. However, we would like to make one comment in this regard. The fact that T_c rapidly grows with the strain and peaks at the strain corresponding to the Lifshits transition (where the γ band touches the X-point) can be explained by either the DOS effect (van Hove singularity) or by a change in pairing interaction. The former explanation, as mentioned before, is realistic for singlet, but not triplet pairing symmetries. The latter would be viable if the change in DOS were sufficient to shift the balance between the AF and FM tendencies toward the latter. To verify that, we have repeated the calculations of the Heisenberg parameters in the strained case. However, we found that the main effect of the strain is not related to the van Hove singularity, and that the average exchange coupling does not become more ferromagnetic. Instead, the strain introduces a splitting between J_{1a} and J_{1b} , while the average value barely changes.

To summarize, we presented first principle calculations of the leading isotropic and anisotropic magnetic interactions in Sr_2RuO_4 . Our results indicate that rotating a p -wave superconducting order parameter during measurements of the Knight shift is impossible by several or-

ders of magnitude and thus the invariance of the Knight shift across the transition remains an unresolved puzzle. We further proposed a model framework, based on a double-exchange type Hamiltonian, and incorporating the calculated magnetic interactions in their entirety, and present an example of using this framework for addressing superconducting pairing symmetry.

METHODS

First principles calculations

For relativistic total energy calculations we have employed the projector augmented wave method [46] as implemented in the Vienna Ab initio Simulation Package (VASP) [47], including SO coupling [48]. We have used the density functional theory within the Perdew-Burke-Ernzerhof parametrization for the exchange and correlation potential [49], and the experimental lattice structure is employed in all calculations. The energy cutoff was set to 400 eV with convergence criteria of 10^{-6} eV. We used up to 1386 irreducible k-points, reduced to 900 for the four formula units cell. For Ru, a pseudopotential with p -states includes as valence states was selected.

For the calculation of the isotropic exchange constants we used the Korringa-Kohn-Rostokker KKR method within the atomic sphere approximation (ASA) [50] and the Green function based magnetic-force theorem [51]. The implementation of this technique has been described elsewhere [52]. Physically, this technique can be considered to be a magnetic analogue of the disordered alloys theory based on coherent potential approximation [52] and is known as the Disordered Local Moments (DLM) approximation [37, 53]. Upon fixing the Ru magnetic moments in the DLM state we achieved self-consistency using 115 irreducible k-points in the Brillouin zone, and then used an extended set of k-points (1529) to compute the isotropic exchange constants in the framework of the magnetic force theorem.

Fitting procedure. The full equation used to describe the calculated energies, including all bilinear terms up to the second neighbors, reads:

$$H_r = \sum_i K(M_i^z)^2 + \sum_{\langle nn \rangle} J_1^{zz} M_i^z M_j^z + \sum_{\langle 100 \rangle} J_1^{xy} (M_i^x M_j^x - M_i^y M_j^y) + \sum_{\langle 010 \rangle} J_1^{xy} (M_i^y M_j^y - M_i^x M_j^x) \quad (6)$$

$$+ \sum_{\langle nmn \rangle} J_2^{zz} M_i^z M_j^z + \sum_{\langle 110 \rangle} J_2^{xy} (M_i^x M_j^x - M_i^y M_j^y) + \sum_{\langle 1\bar{1}0 \rangle} J_2^{xy} (M_i^y M_j^y - M_i^x M_j^x) \quad (7)$$

Here we included for completeness the single-site

anisotropy term K ; since it always enters in the same

TABLE III: Energies of various calculated magnetic states and the corresponding coefficients in Eq. 6. Magnetic moments are described as $\mathbf{M}_{ijk} = \text{Re}[m\mathbf{A} \exp(-i\mathbf{R}_{ijk} \cdot \mathbf{q}_3)]$.

		\mathbf{A}	m	
spiral	planar	$\{1, -i, 0\}$	1	0
	rolling	$\{\frac{i}{\sqrt{2}}, \frac{i}{\sqrt{2}}, 1\}$	1	$(K - J_{zz})/2 + J_2^{zz}/4 - 3J_2^{xy}/4$
	transverse	$\{\frac{i}{\sqrt{2}}, \frac{-i}{\sqrt{2}}, 1\}$	1	$(K - J_{zz})/2 + J_2^{zz}/4 + 3J_2^{xy}/4$
collinear	(110)	$\{\frac{i}{\sqrt{2}}, \frac{i}{\sqrt{2}}, 0\}$	$\sqrt{2}, 1/\sqrt{2}$	$-3J_2^{xy}/2$
	(100)	$\{-1, 0, 0\}$	$\sqrt{2}, 1/\sqrt{2}$	0
	(001)	$\{0, 0, -1\}$	$\sqrt{2}, 1/\sqrt{2}$	$K - J_{zz} + J_2^{zz}/2$

combination with J^{zz} , they cannot be decoupled within this set of calculation. While this term is, in principle, allowed because of itinerancy, we note that the calculated magnetization is close to the the $S = 1/2$ and therefore we expect $K \ll J^{zz}$. This approximation was used in the main text. We also included, besides the nearest neighbor anisotropic interaction J_1^{zz} and J_1^{xy} , the corresponding second nearest neighbor interactions J_2^{zz} and J_2^{xy} . The latter distinguishes between the collinear state polarized along the (110) tetragonal direction and the one polarized along (100)i, and the transverse and rolling spirals. We found it to be relatively small, 0.17 ± 0.05 meV/ μ_B^2 . The second nearest neighbour Kitaev interaction J_2^{zz} simply adds to J^{zz} , and therefore was absorbed into the latter in the fitting procedure. The difference in energies between the planar spiral and the (100) collinear structure, 0.24 meV, is likely related to the fact that the isotropic exchange constants enter these two state differently. Our non-relativistic calculations find them degenerate within the computational accuracy, apparently, fortuitously. Since SOC also affects the isotropic constants, it is no surprise that relativistic effects break this accidental degeneracy.

One can calculate $K - J^{zz}$ and J_2^{xy} either from the set of spiral claculations, or from collinear ones; the results differ by $\pm 30\%$. It is unlikely that this is due to computational inaccuracy, but rather to other interactions not accounted for, such as third neighbors (which is the leading isotropic exchange) or anisotropic biquadratic coupling.

The full summary of the magnetic patterns and their energies used for the fitting, as well as the expressions for the total energies in terms of the parameters in Eq. 7, are presented in Table III.

* These two authors contributed equally

† Electronic address: cesare.franchini@univie.ac.at

- [1] Mackenzie, A. P. and Maeno, Y. The superconductivity of Sr_2RuO_4 and the physics of spin-triplet pairing. *Rev. Mod. Phys.* **75**, 657 (2003).
- [2] Ishida, K. *et al.* Anisotropic pairing in superconducting Sr_2RuO_4 : Ru NMR and NQR studies. *Phys. Rev. B* **56**,

- 505(R) (1997).
- [3] Ishida, K. *et al.* Spin-triplet superconductivity in Sr_2RuO_4 identified by ^{17}O Knight shift. *Nature* **396**, 658 (1998).
- [4] Duffy, J. A. *et al.* Polarized-neutron scattering study of the cooper-pair moment in Sr_2RuO_4 . *Phys. Rev. Lett.* **85**, 5412 (2000).
- [5] Luke, G. M. *et al.* Time-reversal symmetry-breaking superconductivity in Sr_2RuO_4 . *Nature* **394**, 558 (1998).
- [6] Rice, T. M. and Sigrist, M. Sr_2RuO_4 : an electronic analogue of ^3He ? *J. Phys.: Condens. Matter* **7**, L643 (1995).
- [7] Mazin, I. I. and Singh, D. J. Ferromagnetic spin fluctuation induced superconductivity in Sr_2RuO_4 . *Phys. Rev. Lett.* **79**, 733 (1997).
- [8] Mazin, I. I. and Singh, D. J. Competitions in layered ruthenates: ferromagnetism versus antiferromagnetism and triplet versus singlet pairing. *Phys. Rev. Lett.* **82**, 4324 (1999).
- [9] Braden, M. *et al.* Inelastic neutron scattering study of magnetic excitations in Sr_2RuO_4 . *Phys. Rev. B* **66**, 064522 (2002).
- [10] Murakawa, H., Ishida, K., Kitagawa, K., Mao, Z. Q., and Maeno, Y. Measurement of the ^{101}Ru -Knight shift of superconducting Sr_2RuO_4 in a parallel magnetic field. *Phys. Rev. Lett.* **93**, 167004 (2004).
- [11] Xia, J., Maeno, Y., Beyersdorf, P. T., Fejer, M. M., and Kapitulnik, A. High resolution polar Kerr effect measurements of Sr_2RuO_4 : evidence for broken time-reversal symmetry in the superconducting state. *Phys. Rev. Lett.* **97**, 167002 (2006).
- [12] Nelson, K. D., Mao, Z. Q., Maeno, Y., and Liu, Y. Odd-parity superconductivity in Sr_2RuO_4 . *Science* **306**, 1151 (2004).
- [13] Žutić, I. and Mazin, I. Phase-sensitive tests of the pairing state symmetry in Sr_2RuO_4 . *Phys. Rev. Lett.* **95**, 217004 (2005).
- [14] Matano, K., Kriener, M., Segawa, K., Ando, Y., and Zheng, G.-Q. Spin-rotation symmetry breaking in the superconducting state of $\text{Cu}_x\text{Bi}_2\text{Se}_3$. *Nature Physics* **12**, 852 (2016).
- [15] Yonezawa, S., Tajiri, K., Nakata, S., Nagai, Y., Wang, Z., Segawa, K., Ando, Y., and Maeno, Y. Thermodynamic evidence for nematic superconductivity in $\text{Cu}_x\text{Bi}_2\text{Se}_3$. *Nature Physics* doi:10.1038/nphys3907 (2016).
- [16] Yip, S.-K. Models of superconducting $\text{Cu:Bi}_2\text{Se}_3$: Single-versus two-band description. *Phys. Rev. B* **87**, 104505 (2013).
- [17] Fu, L. Odd-parity topological superconductor with nematic order: Application to $\text{Cu}_x\text{Bi}_2\text{Se}_3$. *Phys. Rev. B*

- 90**, 100509(R) (2014).
- [18] Matsumoto, M. and Sigrist, M. Quasiparticle states near the surface and the domain wall in a $p_x \pm ip_y$ -wave superconductor. *J. Phys. Soc. Jpn.* **68**, 994 (1999).
 - [19] Kallin, C. and Berlinsky, A. J. Is Sr_2RuO_4 a chiral p-wave superconductor? *J. Phys. Condens. Matter* **21**, 164210 (2009).
 - [20] Scaffidi, T. and Simon, S. H. Large Chern number and edge currents in Sr_2RuO_4 . *Phys. Rev. Lett.* **115**, 087003 (2015).
 - [21] Kirtley, J. R. *et al.* Upper limit on spontaneous supercurrents in Sr_2RuO_4 . *Phys. Rev. B* **76**, 014526 (2007).
 - [22] Agterberg, D. F. Vortex lattice structures of Sr_2RuO_4 . *Phys. Rev. Lett.* **80**, 5184 (1998).
 - [23] Mineev, V. P. Superconducting phase transition of Sr_2RuO_4 in a magnetic field. *Phys. Rev. B* **89**, 134519 (2014).
 - [24] L.P. Gor'kov, Anisotropy of the upper critical field in exotic superconductors. *JETP Lett.* **40**, 1155 (1984).
 - [25] Amano, Y. Ishihara, M., Ichioka, M., Nakai, N., and Machida, K. Pauli paramagnetic effects on mixed-state properties in a strongly anisotropic superconductor: application to Sr_2RuO_4 . *Phys. Rev. B* **91**, 144513 (2015).
 - [26] Hicks, C. W. *et al.* Strong Increase of T_c of Sr_2RuO_4 Under Both Tensile and Compressive Strain. *Science* **344**, 283 (2014).
 - [27] Hassinger, E. *et al.* Vertical line nodes in the superconducting gap structure of Sr_2RuO_4 . Preprint at <https://arxiv.org/abs/1606.04936> (2016).
 - [28] Ng, K. K. and Sigrist, M. The role of spin-orbit coupling for the superconducting state in Sr_2RuO_4 . *Europhys. Lett.* **49**, 473 (2000).
 - [29] Eremin, I., Manske, D., and Bennemann, K. H. Electronic theory for the normal-state spin dynamics in Sr_2RuO_4 : Anisotropy due to spin-orbit coupling. *Phys. Rev. B* **65**, 220502(R) (2002).
 - [30] Annett, J. F., Györfy, B. L., Litak, G., and Wysokiński, K. I. Magnetic field induced rotation of the d -vector in the spin-triplet superconductor Sr_2RuO_4 . *Phys. Rev. B* **78**, 054511 (2008).
 - [31] Sidis, Y. *et al.* Evidence for incommensurate spin fluctuations in Sr_2RuO_4 . *Phys. Rev. Lett.* **83**, 3320 (1999).
 - [32] Servant, F. *et al.* Magnetic excitations in the normal and superconducting states of Sr_2RuO_4 . *Phys. Rev. B* **65**, 184511 (2002).
 - [33] Braden, M. *et al.* Anisotropy of the incommensurate fluctuations in Sr_2RuO_4 : a study with polarized neutrons. *Phys. Rev. Lett.* **92**, 097402 (2004).
 - [34] Iida, K. *et al.* Inelastic neutron scattering study of the magnetic fluctuations in Sr_2RuO_4 . *Phys. Rev. B* **84**, 060402(R) (2011).
 - [35] de Boer, P. K. and de Groot, R. A. Electronic structure of magnetic Sr_2RuO_4 . *Phys. Rev. B* **59**, 9894 (1999).
 - [36] Glasbrenner, J. K. *et al.* Effect of magnetic frustration on nematicity and superconductivity in iron chalcogenides. *Nature Phys.* **11**, 953 (2015).
 - [37] Györfy, B. L., Pindor, A. J., Staunton, J., Stocks, G. M., and H. Winter. A first-principles theory of ferromagnetic phase transitions in metals. *J. Phys. F: Met. Phys.* **15**, 1337 (1985).
 - [38] Dzyaloshinskii, I. E. A thermodynamic theory of weak ferromagnetism of antiferromagnetics. *J. Phys. Chem. Solids* **4**, 241 (1958).
 - [39] Moriya, T. Anisotropic superexchange interaction and weak ferromagnetism. *Phys. Rev.* **120**, 91 (1960).
 - [40] Haverkort, M. W., Elfimov, I. S., Tjeng, L. H., Sawatzky, G. A., and Damascelli, A. Strong spin-orbit coupling effects on the Fermi surface of Sr_2RuO_4 and Sr_2RhO_4 . *Phys. Rev. Lett.* **101**, 026406 (2008).
 - [41] Veenstra, C. N. *et al.* Spin-orbital entanglement and the breakdown of singlets and triplets in Sr_2RuO_4 revealed by spin-and angle-resolved photoemission spectroscopy. *Phys. Rev. Lett.* **112**, 127002 (2014).
 - [42] Pavarini, E. and Mazin, I. I. First-principles study of spin-orbit effects and NMR in Sr_2RuO_4 . *Phys. Rev. B* **74**, 035115 (2006); Erratum, *Phys. Rev. B* **76**, 079901 (2007).
 - [43] Fatuzzo, C. G. *et al.* Spin-orbit-induced orbital excitations in Sr_2RuO_4 and Ca_2RuO_4 : A resonant inelastic x-ray scattering study. *Phys. Rev. B* **91**, 155104 (2015).
 - [44] Khomskii, D. I. *Basic Aspects of the Quantum theory of Solids*, Cambridge, 2010.
 - [45] Seo, K., Bernevig, B. A., and Hu, J. P. Pairing symmetry in a two-orbital exchange coupling model of oxypnictides. *Phys. Rev. Lett.* **101**, 206404 (2008).
 - [46] Blöchl, P. E. Projector augmented-wave method. *Phys. Rev. B* **50**, 17953 (1994).
 - [47] Kresse, G. and Furthmüller, J. Efficient iterative schemes for *ab initio* total-energy calculations using a plane-wave basis set. *Phys. Rev. B* **54**, 11169 (1996).
 - [48] Steiner, S. Khmelevskiy, S., Marsmann, M., and Kresse, G. Calculation of the magnetic anisotropy with projected-augmented-wave methodology and the case study of disordered $\text{Fe}_{1-x}\text{Co}_x$ alloys. *Phys. Rev. B* **93**, 224425 (2016).
 - [49] Perdew, J. P., Burke, K., and Ernzerhof, M. Generalized gradient approximation made simple. *Phys. Rev. Lett.* **77**, 3865 (1996).
 - [50] Ruban, A. V. and Skriver, H. L. Calculated surface segregation in transition metal alloys. *Comp. Mater. Sci.* **15**, 199 (1999).
 - [51] Liechtenstein, A. I., Katsnelson, M. I., Antropov, V. P., and Gubanov, V. A. Local spin density functional approach to the theory of exchange interactions in ferromagnetic metals and alloys. *J. Magn. Magn. Mater.* **67**, 65 (1987).
 - [52] Ruban, A. V., Shallcross, S., Simak, S. I., and Skriver, H. L. Atomic and magnetic configurational energetics by the generalized perturbation method *Phys. Rev. B* **70**, 125115 (2004).
 - [53] Cyrot, M. Phase transition in Hubbard model. *Phys. Rev. Lett.* **25**, 871 (1970).

Acknowledgements

B.K, S.K, and C.F were supported by the joint FWF and Indian Department of Science and Technology (DST) project INDOX (I1490-N19), and by the FWF-SFB Vi-CoM (Grant No. F41). I.I.M. is supported by ONR through the NRL basic research program.

Author contributions

S.K. and I.M conceived the research; B.K has carried out most of the numerical calculations with contribution by S.K. and I.M; the superconductivity-related discussion was authored by D.A. and I.M. All authors participated in the discussion and contributed to writing the paper; C.F.

supervised the Vienna part of the project.

Competing financial interests

The authors declare no competing financial interests.